ELSEVIER

Journal of Nuclear Materials 247 (1997) 315–321

journal of nuclear materials

Study on the hydrogen solubility in zirconium alloys

Shinsuke Yamanaka *, Masanobu Miyake, Masahiro Katsura

Department of Nuclear Engineering, Graduate School of Engineering, Osaka University, Yamadaoka 2-1, Suita, Osaka 565, Japan

Abstract

Pure zirconium and zirconium alloys of Zircaloy-2 (1.47 wt% Sn, 0.14 wt% Fe, 0.11 wt% Cr, 0.05 wt% Ni), Zircaloy-4 (1.52 wt% Sn, 0.21 wt% Fe, 0.11 wt% Cr) and Zr–1 wt% Nb alloy and Zr(O) alloys were selected as specimens. The hydrogen solubility measurement was performed in the temperature range 500–1050°C at a hydrogen pressure below 10^4 Pa. The hydrogen solubilities were different among alloys and the phase relationships were affected by the alloying element. The partial thermodynamic quantities of hydrogen in the alloys were derived from the experimental data and the effect of the alloying element was discussed. © 1997 Elsevier Science B.V.

1. Introduction

Zirconium alloys such as Zircaloy have been widely used as the cladding materials of light water reactors. In recent years, hydrogen behavior in the cladding has been watched with keen notice because of high burn up of nuclear fuel required from the economic point of view. The renewed interest in hydrogen embrittlement of the cladding promotes reassessment of the zirconium–hydrogen system.

The hydrogen solubility and the phase diagram for the zirconium–hydrogen binary system have extensively been studied [1–8] and reviewed [9–11]. The phase boundary between the alpha phase and the hydride phase was examined for zirconium alloys below 500°C [12,13]. However, there exists insufficient data for the hydrogen solubility in zirconium alloys at higher temperatures and a little information is available for the effect of gaseous contaminants (mainly H_2O and O_2) on the hydrogen solubility [14]. The hydrogen solubility and the phase diagram are important factors for the practical uses of zirconium alloys in light water reactors under accidental as well as normal operating conditions. From this point of view, the hydrogen solubility in substitutional and interstitial zirconium alloys has been therefore examined in the present study.

* Corresponding author. Tel.: +81-6 789 7887; fax: +81-6 873 3696; e-mail: yamanaka@nucl.eng.osaka-u.ac.jp.

2. Experimental

Zircaloy-2, Zircaloy-4 and Zr–1 wt% Nb, the compositions of which are shown in Table 1, were chosen as substitutional alloys and Zr(O) alloys with an oxygen content of 0.025–0.02 O/Zr were chosen as interstitial alloys. Hydrogen gas (initial purity, 99.999%) was further purified by passing through a hot titanium bed and used for solubility measurement.

The hydrogen solubility was measured in the temperature range 500–1050°C at a hydrogen pressure below 10^4 Pa using a modified Sieverts' apparatus.

3. Results and discussion

3.1. The effect of substitutional element

Figs. 1–8 show the equilibrium hydrogen pressure P_{H_2} (Pa)–hydrogen concentration, C_H (H/Zr atom ratio), isotherms for pure zirconium, Zircaloy-2, Zircaloy-4 and Zr–1 wt% Nb. The following phases appear: hcp α phase, bcc β phase and fcc δ.

The hydrogen solubility in pure zirconium is known to obey Sieverts' law in low hydrogen concentration region. For zirconium alloys, Sieverts' law also holds between the hydrogen pressure and the hydrogen concentration in both the α phase and β phase regions, as shown in Figs. 1–8. In our previous study [15], a comparison of Sieverts'

PII S0022-3115(97)00101-3

Table 1
Compositions of zirconium alloys used in the present study

	Zr [a]	Zircaloy-2	Zircaloy-4	Zr-1Nb
Sn	–	1.47 wt%	1.52 wt%	–
Fe	74 ppm	0.14 wt%	0.21 wt%	530 ppm
Cr	–	0.11 wt%	0.11 wt%	–
Ni	–	0.05 wt%	< 35 ppm	–
Nb	–	–	–	0.97 wt%
O	< 50 ppm	0.125 wt%	0.125 wt%	0.143 wt%
Zr	bal.	bal.	bal.	bal.

[a] Total impurity concentration < 210 ppm.

constant and the enthalpy of solution has been made among zirconium alloys. In the α phase region (below 850°C), Zircaloy-4 had the largest solubility among the alloys and pure zirconium. The enthalpies of solution for the alloys were higher than that for pure zirconium. In the β phase region (above 950°C), the hydrogen solubilities in the alloys were smaller than that in pure zirconium. The enthalpies of solution for the alloys were appreciably higher than that for pure zirconium.

At higher hydrogen concentration, there exist discontinuities in the slope of isotherms below 850°C for pure zirconium, as evidenced by Fig. 1. The discontinuities indicate the phase boundaries: α phase/β phase, β phase/δ phase and α phase/δ phase. Above 900°C, the slope of the isotherm is found from Fig. 2 to vary gradually with the hydrogen concentration, which suggests the existence of a single β phase. There is not a large discrepancy between our results of the phase boundaries and the assessed phase diagrams in the literature [9–11]. The temperature of the eutectoid reaction: $\beta Zr = \alpha Zr + \delta ZrH_{2-x}$ appears to be slightly higher than the 550°C reported in the literature [9–11].

The discontinuities in the slopes of the isotherms for zirconium alloys were observed at the hydrogen concentra-

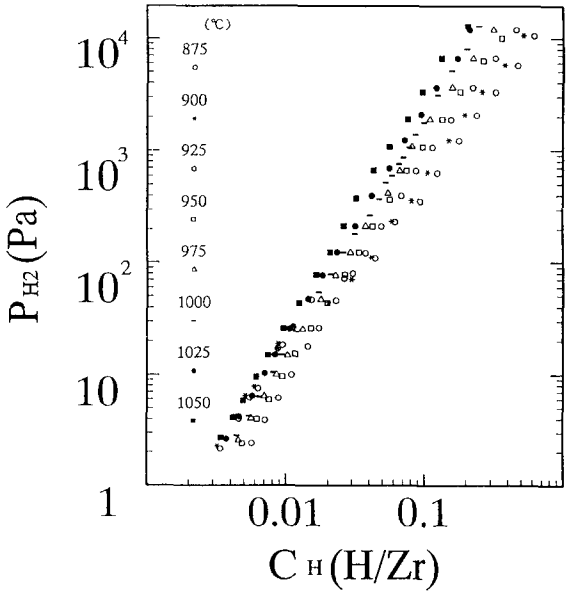

Fig. 2. Equilibrium hydrogen pressure P_{H_2}–hydrogen concentration, C_H, isotherms for pure Zr. (Temperature: 875–1050°C.)

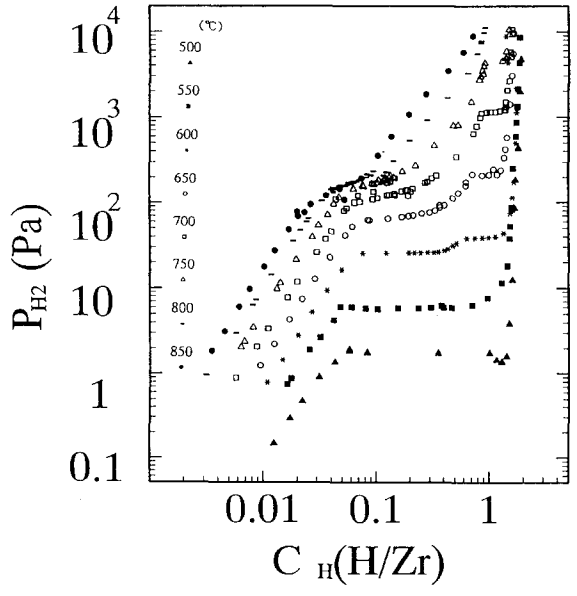

Fig. 1. Equilibrium hydrogen pressure P_{H_2}–hydrogen concentration, C_H, isotherms for pure Zr. (Temperature: 500–850°C.)

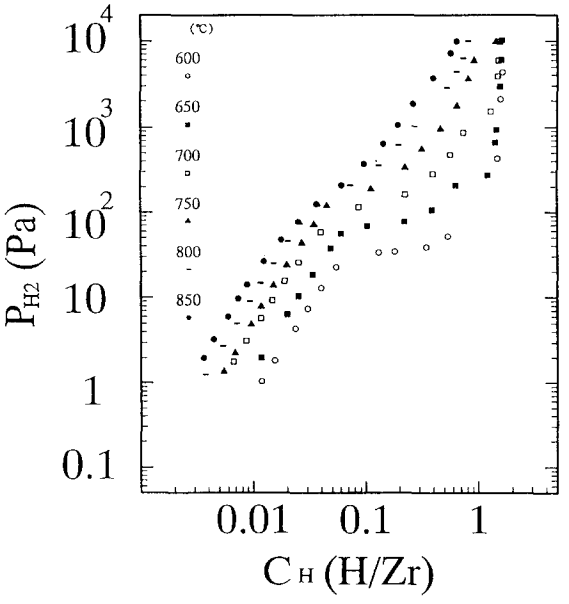

Fig. 3. Equilibrium hydrogen pressure P_{H_2}–hydrogen concentration, C_H, isotherms for Zircaloy-2. (Temperature: 600–850°C.)

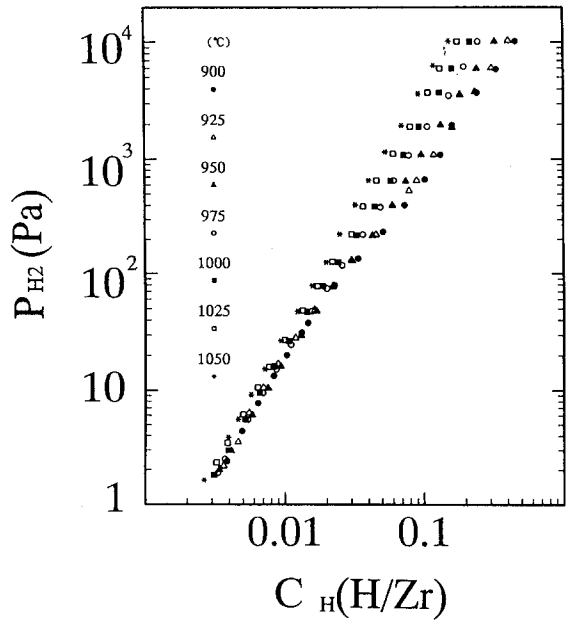

Fig. 4. Equilibrium hydrogen pressure P_{H_2}–hydrogen concentration, C_H, isotherms for Zircaloy-2. (Temperature: 900–1050°C.)

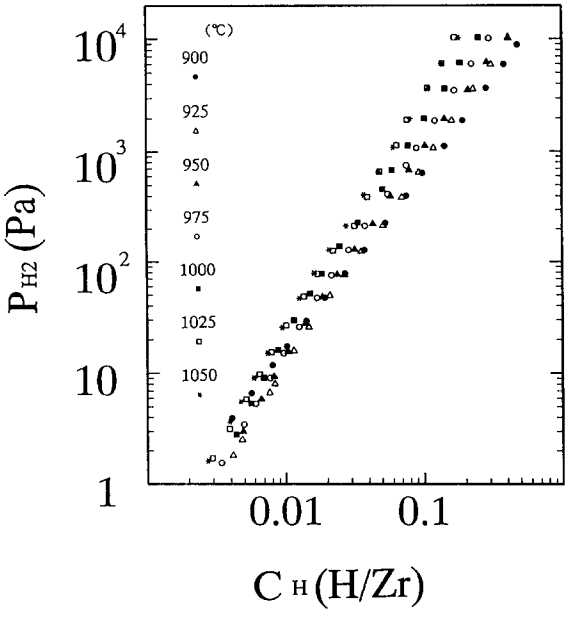

Fig. 6. Equilibrium hydrogen pressure P_{H_2}–hydrogen concentration, C_H, isotherms for Zircaloy-4. (Temperature: 900–1050°C.)

tion above 0.04H/Zr. No plateau pressure was found in the isotherms for zirconium alloys. The regions above 0.04H/Zr appear to correspond to $\alpha + \beta$ phase region. Fig. 9 shows the experimental results obtained for the phase boundaries between the α phase region and the $\alpha + \beta$ phase region for the zirconium alloys (○: Zry-2, △: Zry-4, ●: Zr–1Nb), together with the zirconium–hydrogen system (the dashed line and □). The dotted line indicates the phase boundaries of the Zr–H system [10] and the broken line indicates the reported values for zirconium alloys [12,13]. The phase boundary slightly

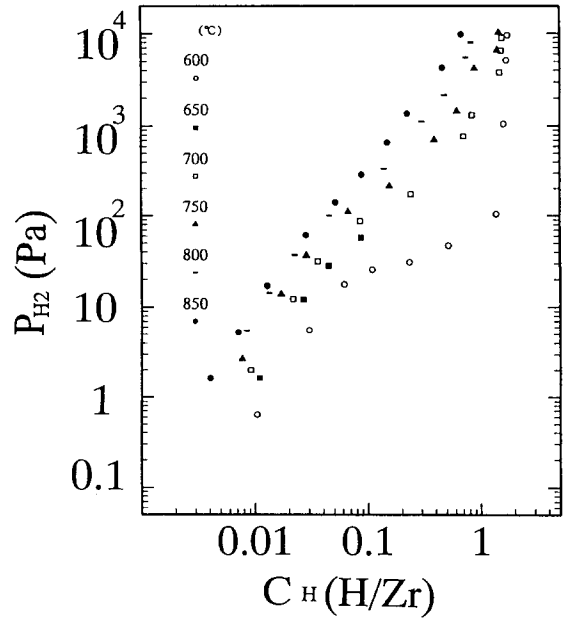

Fig. 5. Equilibrium hydrogen pressure P_{H_2}–hydrogen concentration, C_H, isotherms for Zircaloy-4. (Temperature: 600–850°C.)

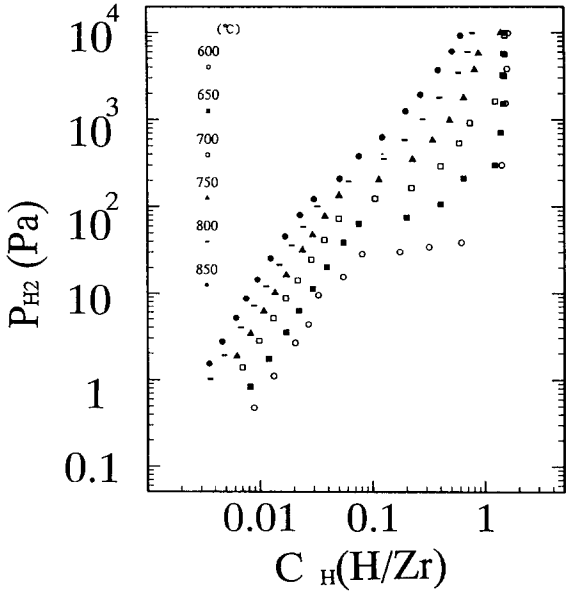

Fig. 7. Equilibrium hydrogen pressure P_{H_2}–hydrogen concentration, C_H, isotherms for Zr–1 wt% Nb. (Temperature: 600–850°C.)

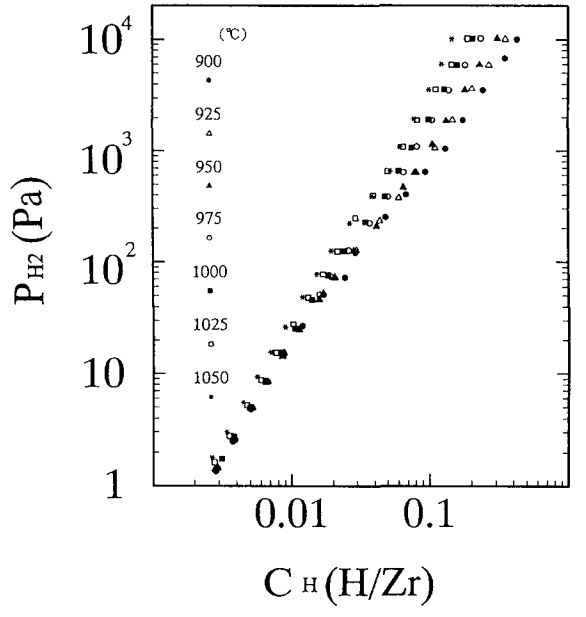

Fig. 8. Equilibrium hydrogen pressure P_{H_2}–hydrogen concentration, C_H, isotherms for Zr–1 wt% Nb. (Temperature: 900–1050°C.)

differs among alloys and the addition of alloying elements such as Sn, Fe, Cr, Ni and Nb appears to increase the stability of the α phase. The effect of each alloying on phase stability has not been clarified in the present study. Our data appear to be consistent with low temperature data sets for zirconium alloys [12,13]. Though the isotherms for the alloys shown in Figs. 1–8 suggest that the phase regions of β, β, +δ and δ may exist in the systems, the phase boundaries at higher hydrogen concentrations were not able to be determined in the present study.

The hydrogen solubility obviously changed with the kind of alloy. Assuming that hydrogen atoms have access to tetrahedral interstitial sites in a zirconium metal lattice, we applied the following solubility equation [16] to the experimental data to analyze the hydrogen solubility in the zirconium alloys:

$$\ln\left(C_H T^{7/4}/(\beta - C_H) P_{H_2}^{1/2} A_{H_2}\right) = -(H_H - E_d)/kT + S_H/k.$$

In this equation, H_H and S_H are the partial molar enthalpy and the partial molar excess entropy of hydrogen ,referring to the standard state of hydrogen atoms at rest in a vacuum, E_d is one half of the dissociation energy of the hydrogen molecule, k the Boltzmann constant and A_{H_2} the value related to partition functions of hydrogen gas. The value of β is the number of interstitial sites of a given kind available to hydrogen per zirconium atom. For the β phase, $\beta = 6$ and for the α phase, $\beta = 2$. In our previous study [15], the values of partial molar thermodynamic

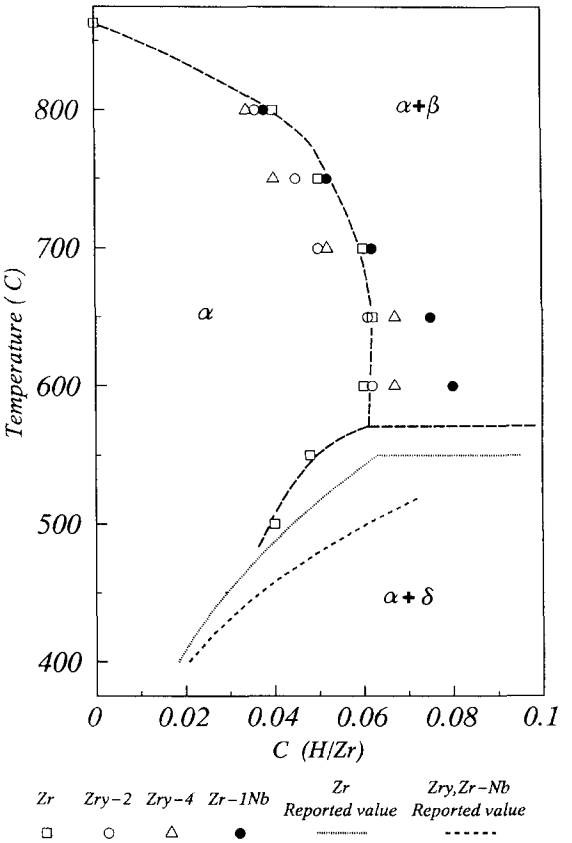

Fig. 9. Phase boundaries between α and α + β for pure Zr and Zr alloys. Experimental values: –□–: Zr, ○: Zry-2, △: Zry-4, ●: Zr–1Nb. Reported values: · · ·, Zr [10], ---, zirconium alloys [12,13].

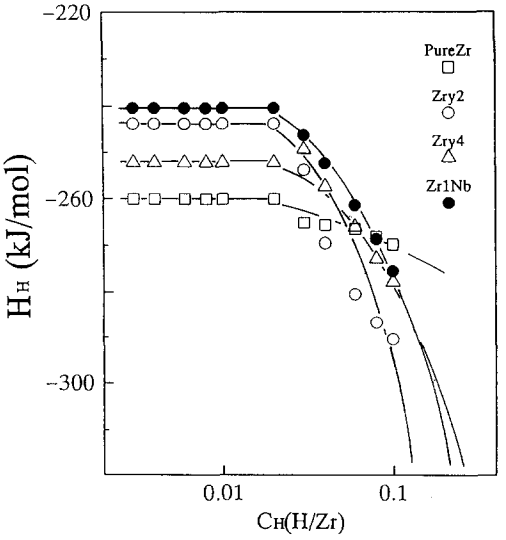

Fig. 10. Change in the partial molar enthalpy H_H value with the hydrogen concentration C_H.

quantities were estimated for the or phase of the alloys and found to be constant irrespective of the hydrogen concentration. The partial molar quantities for the α phase differed among the alloys. The results for the β phase obtained in the present study are indicated in Figs. 10 and 11. As can be seen in Figs. 10 and 11, the partial molar enthalpy and the partial molar excess entropy are constant below 0.02 H/Zr and decrease with increasing hydrogen concentration. The values of the partial molar quantities vary with the kind of alloy and there is a marked difference in the concentration dependence among the alloys.

For both the α and β phases, both the partial molar enthalpy and excess entropy for dilute solution regions increase with the addition of an alloying element. For the α phase, the magnitude of the changes in the partial molar quantities is slightly larger for Zircaloy-4 than for the other alloys, while for the β phase, it is larger for Zr–Nb than for the other alloys. Hydrogen–hydrogen interaction appears to cause the reduction in partial molar quantities for the β phase and the magnitude of the interaction seems to strongly depend on the kind of alloy. The positive changes in the partial molar quantities with addition of alloying elements cannot be explained by vibrational or dilatometric contribution. Further analysis is required to understand the effect of each alloying element on the hydrogen solubility in zirconium.

3.2. The effect of interstitial element

In our previous work [16], thermodynamic studies have been performed on the hydrogen solubility in the hcp αZr(O) alloy. The hydrogen solubility for the hcp α phase first increased with the oxygen content and then decreased at higher oxygen contents. The presence of interstitial oxygen varied the enthalpy of solution.

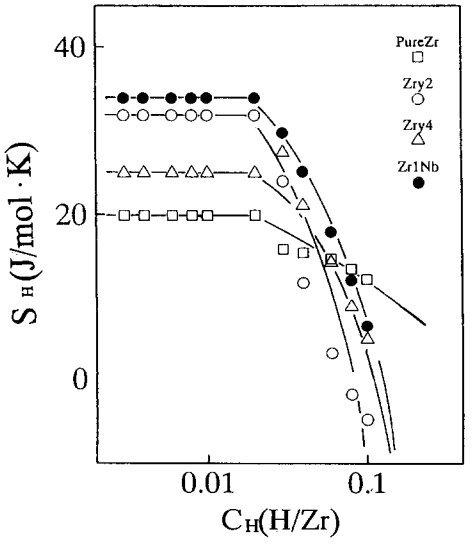

Fig. 11. Change in the partial molar excess entropy S_H value with the hydrogen concentration C_H.

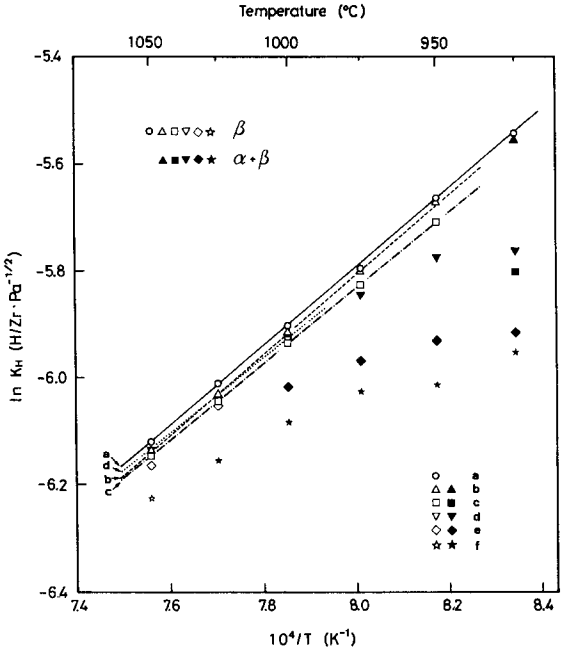

Fig. 12. Temperature dependence of Sieverts' constant K_H for βZr(O) alloys. (a) Pure Zr, (b) 0.0025 O/Zr, (c) 0.0058 O/Zr, (d) 0.0102 O/Zr, (e) 0.0154 O/Zr and (f) 0.0203 O/Zr.

All the solubility data for the bcc βZr(O) closely obey Sieverts' law. The temperature dependence of Sieverts' constant obtained for the βZr(O) alloys is shown in Fig. 12. It is found from Fig. 12 that linear relationships between the natural logarithm of Sieverts' constant and the reciprocal temperature hold for βZr(O) alloys with oxygen contents below 0.01 O/Zr. There is no linear relationship for alloys with higher oxygen contents. This suggests that the Zr(O) alloys below 0.01 O/Zr is the single β phase and the Zr(O) alloys with higher oxygen contents are in the two phase region of α + β. The solubility of hydrogen first decreases with the oxygen content and then increases slightly. This trend for βZr(O) differs from that for αZr(O). The enthalpy of solution first decreases and then increases as the oxygen content increases.

In order to clarify the influence of interstitial oxygen, the solubility data for αZr(O) alloys were analyzed by a dilute solution model proposed for the αZr(O) alloy in our previous study [17]. The changes in the solubility and in the enthalpy of solution with addition of interstitial oxygen were discussed in terms of the difference in partial molar enthalpy and excess entropy between pure metal and alloy, which are defined as, $\delta H = H_H - H_H^0$ and $\delta S = S_H S_H^0$ where H_H and S_H are the partial molar enthalpy and the partial molar excess entropy of hydrogen in βZr(O) and H_H^0 and S_H^0 are the values for pure β zirconium. Figs. 13

and 14 show the changes in δH and δS values with the composition of the alloy. As shown in Figs. 13 and 14, the δH and δS first decrease with the oxygen content and then markedly increase at higher oxygen contents. The change in the solubility in βZr(O) alloys is attributable to a net result from the variation in δH and δS. The effects of interstitial oxygen on partial molar quantities are significantly different from bcc βZr(O) to hcp αZr(O).

On the assumption that the enthalpy and entropy difference δH and δS were given in the form of $\delta H = \delta H^{v} + \delta H^{d} + \delta H^{c}$ and $\delta S = \delta S^{v} + \delta S^{d} + \delta S^{c}$ where δH^{v} and δS^{v} are the differences in vibrational contribution between the alloy and pure zirconium, δH^{d} and δS^{d} the lattice dilatation terms and δH^{c} and δS^{c} the configurational terms, we analyzed the changes in δH and δS with the oxygen content in βZr(O). The results for the analysis are shown in Figs. 13 and 14. Detailed methods for the analysis were published elsewhere [17].

As shown in Figs. 13 and 14, the δH^{v} is small and negative and δS^{v} is small and positive. The values of δH^{v} and δS^{v} obtained for βZr(O) are larger than those for αZr(O). As evidenced by Figs. 13 and 14, the volume expansion due to interstitial oxygen results in a negative enthalpy change and the value of δS^{d} is negligibly small. There is no marked difference in the volume effect between βZr(O) and αZr(O). The configurational enthalpy term δH^{c} increases with the oxygen content, as shown in Fig. 13. Fig. 14 indicates that δS^{c} shows a negative value and decreases with the oxygen content. The trend in δH^{c} and δS^{c} for βZr(O) is almost the same as αZr(O). Although the theoretical curves shown by solid lines in Figs. 13 and 14 demonstrate the tendency for the changes in the experimental δH and δS values with oxygen addition into βZr(O), the absolute values of δH and δS were different from one another.

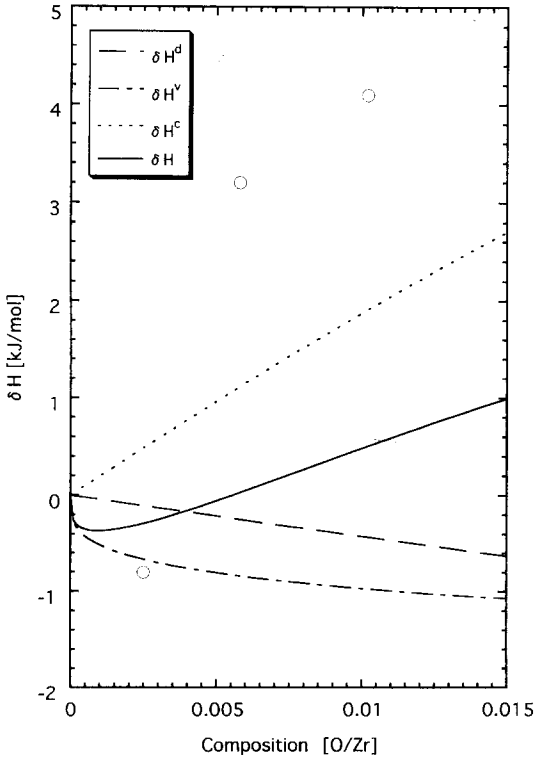

Fig. 13. Theoretical analysis of the change in the δH value with the oxygen content of βZr(O). ○: experimental values.

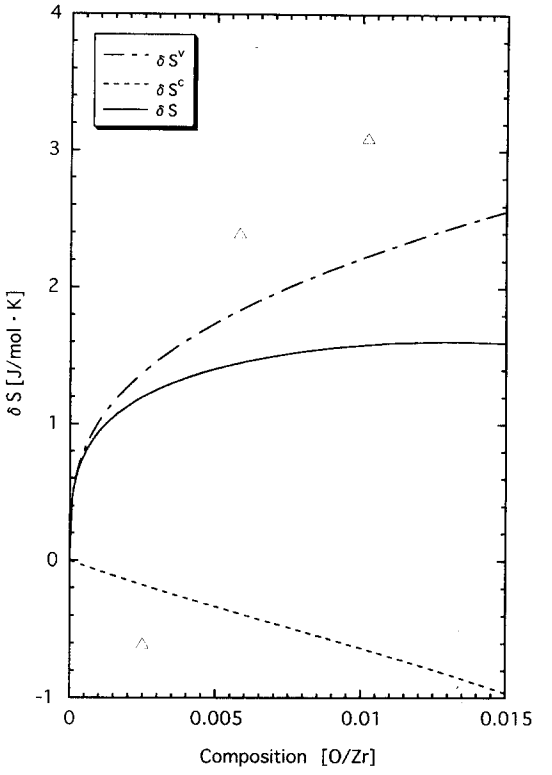

Fig. 14. Theoretical analysis of the change in the δS value with the oxygen content of βZr(O). △: experimental values.

Although we have attempted to account for the influence of interstitial oxygen on hydrogen solubility in zirconium, it is not yet fully clarified. To explain the hydrogen solubility in βZr(O), we have to take into account other contributions such as the dual site occupation of hydrogen in the bcc lattice. The dual site occupation of hydrogen appears to result in increases in δH^{c} and δS^{c}.

4. Conclusion

The hydrogen solubility in pure zirconium and zirconium alloys of Zircaloy-2, Zircaloy-4 and Zr–1 wt% Nb and Zr(O) alloys has been studied to elucidate the influence of substitutional and interstitial elements on hydrogen solubility in zirconium. The solubility measurement was

carried out at the temperatures between 500–1050°C at a hydrogen pressure below 10^4 Pa. The hydrogen solubilities were different among zirconium alloys and the phase relationships were affected by the alloying element. The influence of the alloying element was discussed on the basis of the thermodynamic properties of hydrogen in zirconium alloys derived from the experimental data.

Acknowledgements

The present study has been performed under the auspices of the Japan Atomic Energy Research Institute.

References

[1] C.E. Ells, A.D. McQuillan, J. Inst. Met. 85 (1956) 89.
[2] K. Watanabe, J. Nucl. Mater. 136 (1985) 1.
[3] M. Someno, J. Jpn. Soc. Met. 24 (1955) 136.
[4] E.A. Gulbransen, K.F. Andrew, J. Met. 7 (1955) 136.
[5] M.W. Mallet, W.M. Albrecht, J. Electrochem. Soc. 104 (1957) 142.
[6] R. Rica, T.A. Giorgi, J. Phys. Chem. 71 (1967) 3627.
[7] M. Tada, Y.C. Haung, Titanium–Zirconium 19 (1971) 260.
[8] M. Nagasaka, T. Yamashina, J. Less Common Met. 45 (1976) 53.
[9] E. Zuzek, Surf. Coating Technol. 28 (1986) 323.
[10] E. Zuzek, Bull. Alloy Phase Diagrams 11 (1990) 385.
[11] W.-E. Wang, D.R. Olander, J. Am. Ceram. Soc. 78 (1995) 3323.
[12] D. Hardie, W.H. Erickson, J. Nucl. Mater. 13 (1964) 254.
[13] J.J. Kearns, J. Nucl. Mater. 22 (1967) 292.
[14] M. Moalen, D.R. Olander, J. Nucl. Mater. 178 (1991) 161.
[15] S. Yamanaka, Y. Kashiwara, M. Miyake, J. Alloys Compounds 231 (1995) 730.
[16] S. Yamanaka, T. Tanaka, M. Miyake, J. Nucl. Mater. 167 (1989) 231.
[17] S. Yamanaka, M. Miyake, J. Nucl. Mater. 201 (1993) 134.